Identification of the Proton Pathway in Bacterial Reaction Centers: Decrease of Proton Transfer Rate by Mutation of Surface Histidines at H126 and H128 and Chemical Rescue by Imidazole Identifies the Initial Proton Donors†

Pia Ädelroth,‡,§ Mark L. Paddock,‡ Ali Tehrani,|| J. Thomas Beatty,|| George Feher,‡ and Melvin Y. Okamura*,‡

Department of Physics 0319, 9500 Gilman Drive, University of California San Diego, La Jolla, California 92093, and Department of Microbiology and Immunology, University of British Columbia, Vancouver, Canada, V6T 1Z3

Received July 31, 2001; Revised Manuscript Received September 27, 2001

ABSTRACT: The pathway for proton transfer to Q_B was studied in the reaction center (RC) from *Rhodobacter sphaeroides*. The binding of Zn^{2+} or Cd^{2+} to the RC surface at His-H126, His-H128, and Asp-H124 inhibits the rate of proton transfer to Q_B, suggesting that the His may be important for proton transfer [Paddock, M. L., Graige, M. S., Feher, G. and Okamura, M. Y. (1999) *Proc. Natl. Acad. Sci. U.S.A. 96*, 6183−6188]. To assess directly the role of the histidines, mutant RCs were constructed in which either one or both His were replaced with Ala. In the single His mutant RCs, no significant effects were observed. In contrast, in the double mutant RC at pH 8.5, the observed rates of proton uptake associated with both the first and the second proton-coupled electron-transfer reactions $k_{AB}^{(1)}$ [$Q_A^{-\bullet}Q_B$—$Glu^- + H^+ \rightarrow Q_A^{-\bullet}Q_B$—GluH → $Q_AQ_B^{-\bullet}$—GluH] and $k_{AB}^{(2)}$ [$Q_A^{-\bullet}Q_B^{-\bullet} + H^+ \rightarrow Q_A^{-\bullet}(Q_BH)^\bullet \rightarrow Q_A(Q_BH)^-$], were found to be slowed by factors of ∼10 and ∼4, respectively. Evidence that the observed changes in the double mutant RC are due to a reduction in the proton-transfer rate constants are provided by the observations: (i) $k_{AB}^{(1)}$ at pH ≈ pK_a of GluH became biphasic, indicating that proton transfer is slower than electron transfer and (ii) $k_{AB}^{(2)}$ became independent of the driving force for electron transfer, indicating that proton transfer is the rate-limiting step. These changes were overcome by the addition of exogenous imidazole which acts as a proton donor in place of the imidazole groups of His that were removed in the double mutant RC. Thus, we conclude that His-H126 and His-H128 facilitate proton transfer into the RC, acting as RC-bound proton donors at the entrance of the proton-transfer pathways.

The reaction center (RC)[1] from the photosynthetic bacterium *Rhodobacter* (*Rb.*) *sphaeroides* is a membrane-bound protein complex that catalyzes the light-induced, proton-coupled electron-transfer reactions leading to the reduction and protonation of a bound quinone molecule Q_B ($Q + 2e^- + 2H^+ \rightarrow QH_2$). The RC is composed of three polypeptide subunits (L, M, and H), four bacteriochlorophylls, two bacteriopheophytins, one non-heme iron, and two ubiquinones (UQ_{10}) (reviewed in refs *1* and *2*). Light absorbed by the RC initiates the photoionization of the primary donor, D, a bacteriochlorophyll dimer. The electron is transferred through a bacteriochlorophyll and a bacteriopheophytin to the primary quinone, Q_A, which is the electron donor to Q_B. The protons required for the reduction of the Q_B to quinol are supplied by the aqueous phase on the cytoplasmic side of the membrane. In photosynthetic membranes, the reduced quinol leaves the RC and is oxidized by the bc_1-complex, releasing the quinol protons on the periplasmic side of the membrane. The proton gradient thus formed is used to drive ATP synthesis.

The double reduction of Q_B takes place in two sequential light-induced electron-transfer reactions. The first electron transfer from $Q_A^{-\bullet}$ to Q_B, $k_{AB}^{(1)}$, produces a stable anionic semiquinone $Q_B^{-\bullet}$. No protonation of the semiquinone occurs at this step, but the electron transfer is coupled to protonation of a nearby acid residue Glu-L212 (*3*, *4*) that occurs due to electrostatic interaction with $Q_B^{-\bullet}$. The $k_{AB}^{(1)}$ process has been shown to be independent of the driving force for electron transfer (*5*), from which it was concluded that the rate-limiting step is a conformational change in the RC. $k_{AB}^{(1)}$ decreases with increasing pH >8.5 due to ionization of Glu-L212 (pK_a ≈ 8.5), and the requirement that Glu-L212 be protonated prior to electron transfer (*4*). We represent the $k_{AB}^{(1)}$ reaction as a two-step process shown in eq 1 (*6*):

$$Q_A^{-\bullet}Q_B\text{---}Glu^- + H^+ \underset{(fast)}{\overset{k_{H^+(2)}}{\rightleftharpoons}} Q_A^{-\bullet}Q_B\text{---}GluH \xrightarrow[(slow)]{k_c} Q_AQ_B^{-\bullet}\text{---}GluH \qquad (1)$$

where $k_{H^+(2)}$ is the rate constant of proton uptake of $H^+(2)$ from solution to Glu-L212 and k_c is the rate (∼10^4 s^{-1}) of the conformational change that precedes and limits the rate of electron transfer. In the native RC, the proton-transfer rate $k_{H^+(2)}$ is faster than k_c, resulting in a single exponential for

† This work was supported by the National Science Foundation (Grant MCB 99-82186), the National Institutes of Health (Grant GM-41637 and GM-13191), the Canadian Institutes for Health Research, and by a postdoctoral fellowship from the Swedish Foundation for International Cooperation in Research and Higher Education (STINT) to P.Ä.

* To whom correspondence should be addressed. Phone: (858) 534-2505. Fax: (858) 822-0007. E-mail: mokamura@ucsd.edu.

‡ Department of Physics.

§ Present address: Department of Biochemistry and Biophysics, The Arrhenius Laboratories for Natural Sciences, Stockholm University, SE-106 91 Stockholm, Sweden.

|| Department of Microbiology and Immunology.

[1] Abbreviations: D, primary electron donor; Q_A, primary quinone electron acceptor; Q_B, secondary quinone electron acceptor; Q_{10}, coenzyme Q-10 (2,3-dimethoxy-5-methyl-6-decaisoprenyl-1,4-benzoquinone); RC, reaction center; cyt *c*, horse heart cytochrome *c*.

10.1021/bi011585s CCC: $20.00
Published on Web 11/07/2001

$k_{AB}^{(1)}$ at pH >8 with a rate constant equal to k_c times the fraction of protonated Glu-L212.

The first protonation of the reduced Q_B [uptake of $H^+(1)$] occurs during the second electron transfer, $k_{AB}^{(2)}$. This protonation, to form the intermediate $Q_BH^{-\bullet}$ is energetically unfavorable. $Q_BH^\bullet$ accepts a second electron from $Q_A^{-\bullet}$, which is the rate-limiting step in the $k_{AB}^{(2)}$ process (*7*), shown in eq 2. The second protonation [$H^+(2)$] of reduced Q_B involves internal transfer to $(Q_BH)^-$ from Glu-L212 (*8*), forming Q_BH_2:

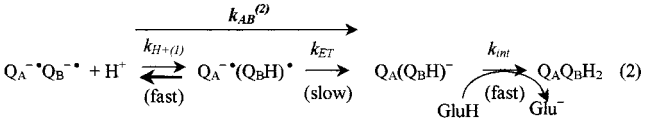

(2)

where $k_{H^+(1)}$ is the rate constant of proton uptake of $H^+(1)$, k_{ET} is the intrinsic rate of electron transfer, and k_{int} is the internal transfer rate of $H^+(2)$ from Glu-L212 to reduced Q_B. In the native RC, $k_{H^+(1)}$ is much faster than $k_{AB}^{(2)}$. Thus, $k_{AB}^{(2)}$ is equal to k_{ET} times the fraction of $Q_BH^\bullet$ ($pK_a \approx 4.5$).

The Q_B molecule is located in the interior of the RC without direct contact with the external solution. Several putative proton-transfer pathways consisting of protonatable amino acids and/or water molecules leading from the cytoplasm to the quinone-binding site have been identified in the crystal structures of the RC (*9*−*11*).

The dominant functional proton-transfer pathway for H^+-(1) has been shown by site-directed mutagenesis to involve Asp-L213 (*3*, *12*−*14*), Ser-L223 (*12*), Asp-L210, and Asp-M17 (*15*, *16*). More recently the entry region for $H^+(1)$ was identified using the inhibitory effect on proton transfer by the metal ions Zn^{2+} and Cd^{2+}, which bind to the surface of the RC at His-H126, His-H128, and Asp-H124 (*17*, *18*).

The transfer of $H^+(2)$ to reduced Q_B has been shown by site-directed mutagenesis to involve internal transfer from Glu-L212 (*3*, *4*). The entrance for proton uptake to Glu-L212 has been shown to be the same as for $H^+(1)$ (*6*), i.e., the region around the metal-binding site His-H126, His-H128, and Asp-H124. The pathway for $H^+(2)$ shares with $H^+(1)$ the involvement of Asp-M17, Asp-L210, and Asp-L213 (*16*), before branching off to Glu-L212.

The inhibitory effect by metal ion binding to His-H126, His-H128, and Asp-H124 on proton transfer to Q_B was proposed to be due to the loss of the imidazole groups of the His as initial proton donors in the proton-transfer pathway (*6*, *18*). However, alternative explanations for the slow proton transfer in the metal-bound RC might be invoked. These include a change of protein dynamics in the Q_B region, or a change in the pK_as of internal acid residues (*19*).

In this work, we investigated the role of the residues His-H126 and His-H128 directly by determining the effect of replacing either one or both of these histidines with alanine. Proton uptake rates and the coupled electron-transfer rates were measured in the mutant RCs to determine the effects of removing the imidazole group of the His at H126 and H128. To assay whether the changes in the measured electron and proton-transfer rates were due to the loss of the proton donor function of the imidazole group, exogenous proton donors such as imidazole were added to the mutant RCs. This strategy to overcome a rate limitation due to a mutation by adding an analogous exogenous molecule to the modified protein ("chemical rescue") has been widely used to investigate the function of specific histidine residues as proton donors/acceptors (see refs *20* and *21* and references therein). A preliminary account of some of this work has been presented (*22*).

MATERIALS AND METHODS

Reagents and Quinones. Q_{10} (2,3-dimethoxy-5-methyl-6-decaisoprenyl-1,4-benzoquinone) was obtained from Sigma, prepared in ethanol, dried under nitrogen and solubilized in 1% LDAO (lauryl-dimethylamine-*N*-oxide). MQ_4 (menatetrenone; 2-methyl-3-tetraisoprenyl-1,4-naphtho-quinone) was from Sigma. Me_4NQ (2,3,6,7-tetramethyl-1,4-naphthoquinone) was kindly provided by J. M. Bruce, University of Manchester, U.K. M-cresol purple was obtained from Sigma. Horse heart cytochrome *c* was obtained from Sigma and reduced (>95%) by hydrogen gas using platinum black as a catalyst. All other reagents were of analytical grade.

Site-Directed Mutagenesis and Preparation of Reaction Centers. The mutants were constructed as described (*23*), except that for the His-H126 → Ala [HA(H126)] and His-H128 → Ala [HA(H128)] substitutions the entire *puhA* gene was sequenced both prior and after conjugation into *Rb. sphaeroides*. This extensive sequencing obviated the need for subcloning the gene segments. The host strain used for expression of mutant genes was a derivative of ΔPUHA (*24*) in which the *pucBA* genes had been disrupted as described (*25*).

RCs from *Rb. sphaeroides* R26.1 and mutant strains were purified to a ratio A^{280}/A^{800} of ≤1.3 in LDAO as described (*26*). The Q_B-site was reconstituted by addition of 3−4-fold excess Q_{10} in 1% LDAO, followed by dialysis against 15 mM Tris, 0.1 mM EDTA, and 0.04% β-D-dodecylmaltoside.

Substitution of Q_{10} in the Q_A site with different naphthoquinones for the driving force assay was performed as in ref *27*.

Electron Transfer and Proton Uptake Measurements. Absorbance changes in response to a laser flash were measured using an spectrometer of local design (*28*). Actinic illumination was provided by a Nd:YAG laser (Opotek, Carlsbad, CA). Charge recombination k_{BD} ($D^{+\bullet}Q_B^{-\bullet} \rightarrow DQ_B$) and k_{AD} ($D^{+\bullet}Q_A^{-\bullet} \rightarrow DQ_A$) was measured by monitoring the recovery of D at 865 nm. The occupancy of the Q_B site, usually 80%, was determined from the fraction of the slower component of the recombination rate, k_{BD} (*28*). k_{AD} was measured after addition of 100 μM terbutryn, which blocks electron transfer to Q_B. Electron transfer $k_{AB}^{(1)}$ was measured by monitoring the bacteriopheophytin band-shift at 750 nm (*29*, *30*) following a single laser flash. The second electron transfer $k_{AB}^{(2)}$ was determined by monitoring the decay of the semiquinone absorption at 450 nm following a second laser flash in the presence of 20 μM horse-heart cytochrome c^{2+} (*31*). Proton uptake was measured at 580 nm after the first and second flashes using 40 μM of the pH-sensitive dye *m*-cresol purple in 50 mM KCl, 0.04% β-D-dodecyl maltoside after removal of buffer as in ref *6*. Electron-transfer measurements were performed in a solution of 50 mM KCl, 0.04% β-D-dodecyl maltoside. Note that buffers were avoided since some buffers, e.g., Tris, had a rescuing effect on proton transfer (and hence electron transfer) rates in the double

Table 1: Measured Electron Transfer Rates for Native and Mutant RCs in the Presence and Absence of Imidazole (pH 8.5, $T = 21$ °C)

			no imidizole		+50 mM imidizole	
RC[a]	k_{AD} (s^{-1})	k_{BD} (s^{-1})	$k_{AB}^{(1)}$ [b] (s^{-1})	$k_{AB}^{(2)}$ [b] (s^{-1})	$k_{AB}^{(1)}$ (s^{-1})	$k_{AB}^{(2)}$ (s^{-1})
native	8	1.0	4×10^3	3.5×10^2	4×10^3	3.5×10^2
HA(H126)	8	1.3	3×10^3	2.8×10^2	3×10^3	2.8×10^2
HA(H128)	8	1.1	3.5×10^3	4×10^2	3.5×10^3	4×10^2
HA(H126)/HA(H128)	8	1.3	5×10^2 [c]	1×10^2 [d]	3.5×10^3	3.5×10^2

[a] HA(H126) = His-H126 → Ala, HA(H128) = His-H128 → Ala, HA(H126)/HA(H128) = His-H126 → Ala/His-H128 → Ala. [b] The proton uptake rates (measured in the same sample), were the same (within 5%) as the electron-transfer rates in the absence of added imidazole. In the presence of added imidazole, proton uptake cannot be measured because of the buffering of the sample. Between samples, the electron-transfer rates vary ±15%. [c] The rate constant refers to the slow, proton-limited phase (see Results). [d] Note that the change in the proton transfer rate is significantly greater than the change in the observed rate; this is because the reaction in the native or rescued systems are not limited by the proton-transfer step.

mutant RC. The pH of samples was controlled by continuous measurements and readjustments.

RESULTS

Charge Recombination k_{AD} ($D^{+\bullet}Q_A^{-\bullet} \rightarrow DQ_A$) and k_{BD} ($D^{+\bullet}Q_B^{-\bullet} \rightarrow DQ_B$). To assay for structural integrity of the RC and stability of $Q_B^{-\bullet}$ (*3*, *4*, *27*, *32*), charge recombinations k_{AD} and k_{BD} were measured in the His-H126 → Ala [HA-(H126)], His-H128 → Ala [HA(H128)], and His-H126 → Ala/His-H128 → Ala [HA(H126)/HA(H128)] mutant RCs. Neither k_{AD} nor k_{BD} were significantly different in any of the mutant RCs compared to the native RC at pH 8.5 (Table 1). The pH dependence of k_{BD} in all the mutant RCs was the same as in the native RC at high (>8.5) and low (<6.5) pH and differed by at most 30% in the intermediate region ($6.5 < pH < 8.5$).

Proton Uptake by Glu-L212: Measurements of $k_{AB}^{(1)}$ ($D^{+\bullet}Q_A^{-\bullet}Q_B^{-}$—$Glu^- + H^+ \rightarrow D^{+\bullet}Q_AQ_B^{-\bullet}$—GluH) and the Associated Proton Uptake Rate. Proton uptake by Glu-L212 was measured in two ways: by directly monitoring proton uptake from solution and by monitoring the coupled electron transfer $k_{AB}^{(1)}$ (eq 1). In the native RC, the proton uptake rate constant and $k_{AB}^{(1)}$ were both ~4000 s^{-1} at pH 8.5 (Figure 1 and Table 1). These rates were not significantly affected in the single mutant RCs HA(H126) and HA(H128) (see Table 1). In contrast, in the double mutant RC HA-(H126)/HA(H128) proton uptake was slowed to ~500 s^{-1} at pH 8.5 (Table 1 and Figure 1B). Electron transfer $k_{AB}^{(1)}$ at pH 8.5 was biphasic in the mutant (Figure 1A), with the faster phase having the native rate constant (4000 s^{-1}), and the slower phase having the same rate as that measured for proton uptake (500 s^{-1}). The fraction of the slow phase increased with increasing pH (Figure 2), with an observed pK_a of ~8.6. Thus, at pH <8 the fraction of slow phase was very small, making the observed kinetics in the mutant the same as in native RCs.

Proton uptake By $Q_B^{-\bullet}$: Measurements of $k_{AB}^{(2)}$ ($DQ_A^{-\bullet}Q_B^{-\bullet} + H^+ \rightarrow DQ_A(Q_BH)^-$) and the Associated Proton Uptake Rate. Proton uptake by $Q_B^{-\bullet}$ was measured in two ways: by directly monitoring proton uptake from solution, and by monitoring the coupled electron transfer $k_{AB}^{(2)}$ (eq 2). These rates were ~350 s^{-1} in the native RC at pH 8.5 (Table 1). No significant effects on $k_{AB}^{(2)}$ were observed in the single mutants HA(H126) and HA(H128) (see Table 1). In contrast, in the double HA(H126)/HA(H128) mutant in the range $7 < pH < 9$, both the proton uptake rate and $k_{AB}^{(2)}$ were decreased[2]; the rates were ~100 s^{-1} at pH 8.5 (Figure 3,-panels A and B and Table 1).

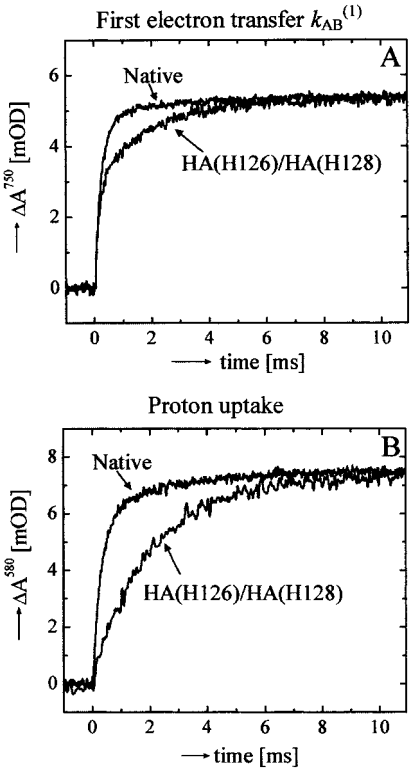

FIGURE 1: Electron transfer (A) and proton uptake (B) associated with the $k_{AB}^{(1)}$ reaction ($Q_A^{-\bullet}Q_B$—$Glu^- + H^+ \rightarrow Q_AQ_B^{-\bullet}$—GluH) (eq 1) in native and HA(H126)/HA(H128) mutant RCs at pH 8.5. (A) Electron transfer was measured at 750 nm which is sensitive to the reduction states of the quinones (*29*, *30*). (B) Proton uptake was measured at 580 nm using the pH-sensitive dye *m*-cresol purple. The buffered signal, measured after addition of 5 mM Tris was subtracted from the traces. The proton uptake traces have been scaled to the same amplitude for clarity. The amplitude of proton uptake in the HA(H126)/HA(H128) mutant RC is ~25% smaller than the amplitude in the native RC at this pH. Note that the observed rates in panels A and B are the same in the native RC, and that the slower phase in panel A is the same as the rate in panel B in the mutant RC. Experimental conditions: 2 μM RC, 50 mM KCl, 0.04% β-D-dodecyl maltoside, 40 μM *m*-cresol purple, pH 8.5, 21 °C, average of ~15 traces.

The dependence of $k_{AB}^{(2)}$ on the driving force for electron transfer was measured in native and double mutant RCs at pH 8.5 by replacing Q_{10} in the Q_A site with either of two naphthoquinones having different redox potentials as described in ref *7*. In the native RC, $k_{AB}^{(2)}$ was dependent on the driving force, increasing ~5-fold when the Q_A site was

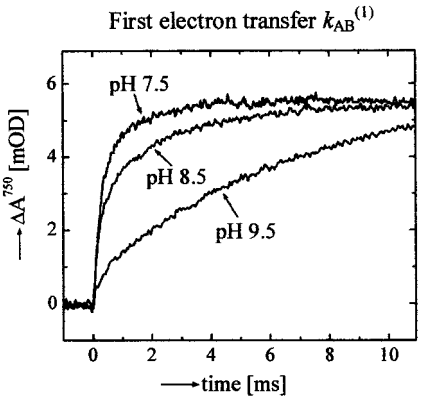

FIGURE 2: Electron transfer $k_{AB}^{(1)}$ in the HA(H126)/HA(H128) mutant RC at pH 7.5, 8.5, and 9.5. Note that the fraction of the observed signal with the slower kinetic rate increases with increasing pH with an apparent p$K_a \approx 8.6$. Experimental conditions: 2 μM RC, 50 mM KCl, 0.04% β-D-dodecyl maltoside, 21 °C, average of ~15 traces.

occupied by Me_3NQ, confirming previous results (*7*). In contrast, in the HA(H126)/HA(H128) mutant RC, $k_{AB}^{(2)}$ was independent of the driving force (Figure 4), showing that electron transfer is not rate-limiting in the double mutant RC.

Chemical Rescue of the Slowed Proton Uptake Rates. To test whether exogenous proton donors could rescue the slow rate of proton uptake in the double mutant HA(H126)/HA(H128) RC, we measured $k_{AB}^{(1)}$ and $k_{AB}^{(2)}$ in the absence and presence of exogenous donors, such as imidazole.

At pH 9, ~80% of the $k_{AB}^{(1)}$ kinetics displayed the slow rate. At this pH, the slow component of $k_{AB}^{(1)}$ decreased from ~1200 s^{-1} (native) to ~200 s^{-1} in the double mutant RC (Figure 5A). This rate was increased by the addition of exogenous imidazole. The rate reached ~85% of the native rate upon addition of ≥50 mM imidazole (Figure 5A). In the presence of 50 mM imidazole, the pH dependence of $k_{AB}^{(1)}$ in the double mutant RC was the same as in the native RC, i.e., monophasic kinetics with the rate decreasing above pH 8.5 (pK_a of Glu-L212; data not shown).

Addition of imidazole had no effect on $k_{AB}^{(1)}$ in native or single His mutant RCs (Table 1). The effect of imidazole in the double mutant RC was reversible such that after removal of imidazole $k_{AB}^{(1)}$ was again ~200 s^{-1}, the same as before addition of imidazole. Addition of salt (KCl) did not increase $k_{AB}^{(1)}$ in either the mutant nor the native RC (data not shown).

Similarly, $k_{AB}^{(2)}$ was increased in the double mutant RC by addition of imidazole. The rate reached native values upon addition of ≥50 mM imidazole (Table 1 and Figure 5B). Upon addition of 50 mM imidazole to the double mutant RC, $k_{AB}^{(2)}$ was dependent on the driving force for electron transfer (Figure 4), showing that the mechanism of $k_{AB}^{(2)}$ had changed to that observed in the native RC. Imidazole had no effect on $k_{AB}^{(2)}$ in native or single His mutant RCs (Table 1).

In contrast to the large effects of imidazole (50 mM) on $k_{AB}^{(1)}$ and $k_{AB}^{(2)}$, it had only small (<30%) effect (similar to addition of KCl) on k_{BD} in the double mutant RC, and even a smaller effect in native and single mutant RCs.

[2] It was previously reported that no effects on $k_{AB}^{(2)}$ were observed in the double mutant RC (*33*). The difference between that observation and the one reported in this work is attributed to the lower pH used (7.5) and the presence of 10 mM Tris buffer in the previous study.

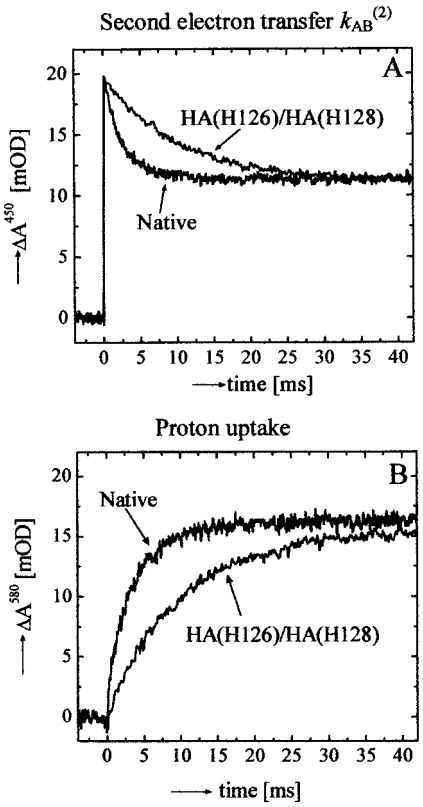

FIGURE 3: Electron transfer (A) and proton uptake (B) associated with the $k_{AB}^{(2)}$-reaction [$Q_A^{-\bullet}Q_B^{-\bullet} + H^+ \rightarrow Q_A(Q_BH)^-$] (eq 2) in native and HA(H126)/HA(H128) mutant RCs. (A) Electron transfer was measured at 450 nm, the peak absorption of the semiquinone species. The initial rise is due to the formation of the $Q_A^-Q_B^-$ state which decays to $(Q_BH)^-$ resulting in the observed transient. The residual absorption at longer times is due to the exogenous electron donor, cyt *c*, which is needed to perform the double flash experiment. (B) Proton uptake was measured at 580 nm using the pH-sensitive dye *m*-cresol purple. The buffered signal, measured with 5 mM Tris, was subtracted from the traces. The proton uptake traces have been scaled to the same amplitude for clarity. The amplitude of proton uptake in the HA(H126)/HA(H128) mutant RC is ~25% larger than the amplitude in the native RC. Note that the observed rates are the same in panels A and B. Experimental conditions: 2 μM RC, 50 mM KCl, 0.04% β-D-dodecyl maltoside, 40 μM *m*-cresol purple (in panel B), 20 μM cyt *c*, pH 8.5, 21 °C, average of ~5 traces.

DISCUSSION

It has been previously shown that the entry region for both protons involved in the reduction of Q_B to Q_BH_2 is located near Asp-H124, His-H126, and His-H128 (*6*, *17*, *18*) at the cytoplasmic surface of the RC. This conclusion was arrived at from the inhibitory effect on proton transfer upon binding Cd^{2+} or Zn^{2+} to these surface residues. In this study, we investigated by site-directed mutagenesis the role of these surface histidines in the proton-transfer process. Two single mutant RCs that lack one of the imidazole groups HA(H126) or HA(H128) and a double mutant that lacks both imidazole groups, HA(H126)/HA(H128), were constructed and the rates of proton uptake from solution and the proton-coupled electron-transfer reactions $k_{AB}^{(1)}$ and $k_{AB}^{(2)}$ were measured. Furthermore, the ability of exogenous imidazole to substitute for the missing histidines was investigated. The implications

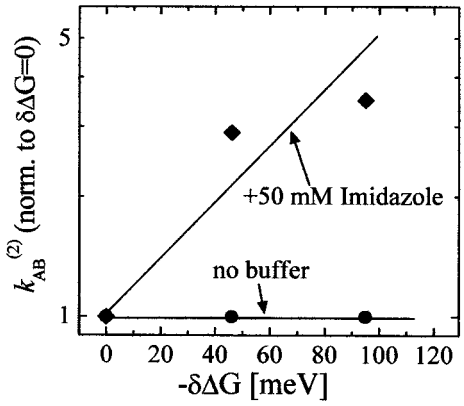

FIGURE 4: Dependence of $k_{AB}^{(2)}$ on the driving force for electron transfer in the HA(H126)/HA(H128) mutant RC in the absence (circles) and presence (diamonds) of 50 mM imidazole. The driving force for electron transfer was changed by replacing the native Q_{10} (defined to be at $\delta\Delta G = 0$) in the Q_A site with naphthoquinones having lower midpoint potentials. The resulting change in slope indicates a change in mechanism (eq 2) from proton transfer-limited (no buffer) to electron transfer-limited (50 mM imidazole). The observed driving force dependence in the native RC (not shown) is similar to the dependence in the mutant in the presence of 50 mM imidazole. Experimental conditions: 2 μM RC, 10 mM KCl, 0.04% β-D-dodecyl maltoside, 20 μM cyt *c*, pH 8.5, 21 °C.

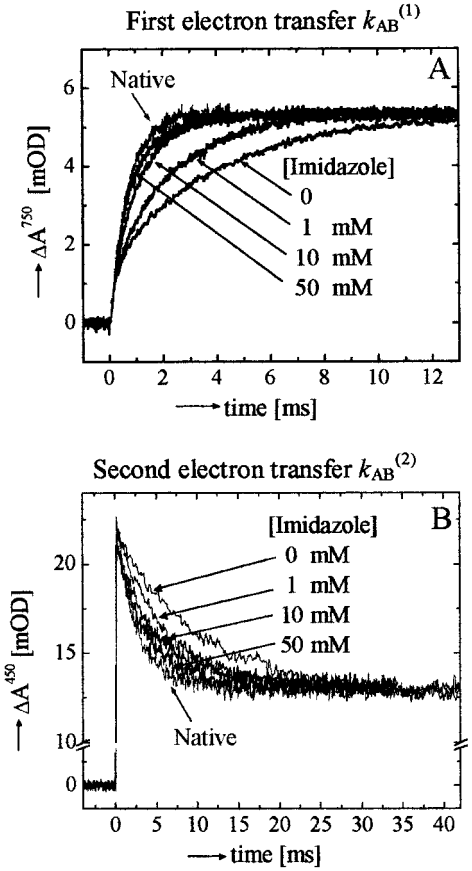

FIGURE 5: "Chemical rescue" by exogenous imidazole of $k_{AB}^{(1)}$ at pH 9 (A) and $k_{AB}^{(2)}$ at pH 8.5 (B) in the HA(H126)/HA(H128) mutant RC. The rescuing effect for $k_{AB}^{(1)}$ was measured at pH 9 because of the larger extent (~80%) of the slow phase. Experimental conditions: 2 μM RC, 50 mM KCl, 0.04% β-D-dodecyl maltoside, 21 °C, average of ~5−20 traces. Note that the rates could be restored to native like rates in the presence of imidazole.

of the results for the role of the histidines in proton transfer are discussed.

Proton Uptake from Solution Is Slowed When Both His-H126 and His-H128 Are Replaced with Ala. Upon replacement of either His-H126 or His-H128 by Ala, no changes in the rates of proton uptake were observed. In contrast, upon replacement of both His by Ala, the rates of proton uptake were decreased 4−10-fold (Table 1). These reductions in the observed proton uptake rates can be explained in terms of loss of the proton-transfer roles of His-H126 and His-H128.

The observed proton-coupled electron-transfer kinetics of $k_{AB}^{(1)}$ in the double mutant RC can be explained by the scheme shown in eq 1 where the proton-transfer rate has become slower than the conformational gating step ($k_{H^+(2)} \ll k_c$). When the pH = pK_a of Glu-L212, eq 1 predicts biphasic kinetics with the two phases having equal amplitudes, but different rates. The fast phase, due to the fraction of RCs with protonated Glu-L212, should have a rate k_c. The slow phase due to RCs with unprotonated Glu-L212 is limited by the proton transfer with rate $k_{H^+(2)}$. The rate of the slow phase should be equal to the proton uptake rate, and the amplitude should increase with increasing pH as Glu-L212 becomes more ionized. The observed rates and amplitudes are in good agreement with this model, using pK_a(Glu-L212) ≈ 8.6, $k_c = 4000\ s^{-1}$ and $k_{H^+(2)} = 500\ s^{-1}$ (pH 8.5). In the native RC, the observed single-exponential decay[3] of $k_{AB}^{(1)}$ indicates that $k_{H^+(2)}$ is larger than the observed $k_{AB}^{(1)}$ of $4000\ s^{-1}$. Thus, in the double mutant RC, $k_{H^+(2)}$ is decreased by at least an order of magnitude compared to the native RC.

The proton and electron-transfer kinetics of $k_{AB}^{(2)}$ in the double mutant RC can be explained by the kinetic scheme shown in eq 2 where the proton uptake rate has become slower than the electron-transfer rate, i.e., $k_{H^+(1)} \ll k_{ET}$. This model is very similar to the model in eq 1 except that the pK_a of the protonated semiquinone (≈4.5) is much lower than the pH. Consequently, negligible amounts of protonated semiquinone ($Q_BH^\bullet$) are present at equilibrium, and therefore, the kinetics are monophasic. Thus, when proton transfer is the rate-limiting step, the observed $k_{AB}^{(2)}$ is equal to $k_{H^+(1)}$ and the measured rate should be independent of the driving force for electron transfer. The results are in good agreement with this model, using $k_{H^+(1)} = 100\ s^{-1}$ (pH 8.5). In the native RC, electron transfer is rate limiting (eq 2), implying that $k_{H^+(1)}$ must be greater than the observed rate of $\sim 350\ s^{-1}$ (at least $10^3\ s^{-1}$). Thus, $k_{H^+(1)}$ is decreased at least an order of magnitude in the double mutant compared to the native RC, similar to the change in $k_{H^+(2)}$ (eq 1).

In general, a decrease in the rates of proton uptake could be due to (i) a slower rate of proton delivery to the entry point of the proton-transfer pathways; (ii) electrostatic changes affecting the pK_as of pathway components or acceptor groups; or (iii) structural changes around the proton acceptors. We exclude possibilities ii and iii for the following reasons. The recombination rate k_{BD} ($D^+{}^\bullet Q_B{}^{-\bullet} \rightarrow DQ_B$) is a measure of the structural integrity of the RC and the stability of $Q_B{}^{-\bullet}$ (*3*, *4*, *27*, *32*); the difference in k_{BD} [4] between the double mutant and native RCs is much smaller than the effects on $k_{H^+(1)}$ and $k_{H^+(2)}$. Therefore, there is no evidence

[3] At pH <7, a second faster phase appears (*5*, *34*), which is dependent on experimental conditions. This phase was small compared to the other phase in our experiments and was, therefore, neglected.

to suggest that there are structural or electrostatic changes at or near the Q_B site that could account for the observed decrease in the rates of proton uptake. We, therefore, attribute the slow rates of proton uptake in the double mutant RC to a slower rate of proton delivery to the entry point of the proton-transfer pathways.

Chemical Rescue of the Slow Rates of Proton Transfer in the HA(H126)/HA(H128) Mutant RC by Exogenous Proton Donors. Conclusive evidence that the proton uptake rates limit both $k_{AB}^{(1)}$ and $k_{AB}^{(2)}$ in the double mutant HA(H126)/HA(H128) RC is provided by the ability of exogenous proton donors, such as imidazole, to increase the observed rates. Both $k_{AB}^{(1)}$ and $k_{AB}^{(2)}$ increase with increasing concentrations of imidazole, reaching 85% of the native rates (Figure 5), indicating that the proton transfer rates have increased sufficiently to be no longer rate limiting. This conclusion is confirmed by the observations that in the presence of 50 mM imidazole (i) $k_{AB}^{(1)}$ is monophasic, showing that k_c (eq 1) has become rate limiting (i.e., $k_{H^+(2)} > k_c$) and (ii) $k_{AB}^{(2)}$ is dependent on the driving force for electron transfer, showing that electron transfer (eq 2) has become rate limiting ($k_{H^+(1)} > k_{ET}$).

By analogy with the discussion presented in the previous section, the increase in the rates observed in the presence of imidazole could in principle be due to (i) an increase in the rate of proton delivery from solution; (ii) pK_a shifts of pathway components or acceptor groups; (iii) structural changes; or (iv) general salt effects. We exclude possibilities ii to iv for the following reasons: pK_a shifts of $Q_B^{-\bullet}$ or Glu-L212 would result in a significant change in k_{BD}, which was not observed. The pK_a of Glu-L212 in the double mutant RC, obtained from the k_{AB} data, was determined to be the same within 0.1 pH units as for the native RC. Structural changes are excluded by the lack of significant changes in k_{BD}, the nativelike rates of $k_{AB}^{(1)}$ and $k_{AB}^{(2)}$, and the lack of imidazole effects in the native RC. Salt effects are not responsible for the increases in rates because the addition of KCl causes no increase (but rather a decrease) in $k_{AB}^{(1)}$ and $k_{AB}^{(2)}$ in the mutant RCs. We therefore attribute the "rescue effect" to an increased rate of proton delivery by the addition of the rescuer.

In support of this conclusion are the findings that (i) the observed rates of $k_{AB}^{(1)}$ and $k_{AB}^{(2)}$ in the double mutant RC depend on the concentration of added imidazole (Figure 5), indicating that the rate of collision between the donor and the RC is partly responsible for the observed rates, and (ii) the second-order proton uptake rate constant is a function of the pK_a of the rescuer (manuscript in preparation). This is analogous to the chemical rescue results obtained in carbonic anhydrase (*37*). In that system, proton transfer from the His-64 to the Zn^{2+}-bound hydroxide is the rate-limiting step, and in the absence of the His side chain, exogenous small proton donors such as imidazoles and pyridines bind to the catalytic cavity, replacing the missing His (*38*). In our case, the situation differs. The mechanism for the chemical rescue can be described by a model involving five steps: (i) transient binding of the protonated buffer, (ii) proton transfer to an intermediate proton acceptor group, followed by (iii) transfer to Glu-L212 (for $k_{AB}^{(1)}$) or $Q_B^{-\bullet}$ for ($k_{AB}^{(2)}$), and (iv) unbinding of the deprotonated buffer and *v*) electron transfer, "locking in" the protonated state. A detailed discussion of these steps will be presented in a forthcoming paper.

The background rates of proton uptake in the double mutant RC in the absence of imidazole can be accounted for by direct transfer of H^+ from solution. The observed $k_{AB}^{(1)}$ of 500 s^{-1} at pH 8.5 gives a diffusional rate of 500 s^{-1}/$10^{-8.5}$ M $= 1.6 \times 10^{11}$ M^{-1} s^{-1}, which is close to the range of $10^{10}-10^{11}$ M^{-1} s^{-1} for H^+-diffusion in water (*39*).

Mechanism of Inhibition of Proton Transfer by His Mutation and Metal Binding. The changes in the rates of proton transfer due to simultaneous replacement of His-H126 and His-H128 with Ala and the chemical rescue by imidazole give strong support for the role of the His residues as proton donors in the proton-transfer chain for both $H^+(1)$ and $H^+(2)$. The slow proton uptake observed in the double mutant HA(H126)/HA(H128) RC is similar to that observed upon binding of Zn^{2+} to the native RC. In both cases, $k_{AB}^{(1)}$ becomes biphasic and $k_{AB}^{(2)}$ independent of the driving-force for electron transfer, a consequence of slowed proton uptake (*6*, *18*). This similarity indicates that the loss of the His as proton donors result in slower proton delivery rates to the internal proton accepting groups.

This conclusion is in contrast to the previous proposal by Utschig et al. (*38*) that ascribe the metal-binding effects on $k_{AB}^{(1)}$ to a change in the conformational gating step k_c (eq 1), which we have shown to be unaffected by metal binding (*6*).

Furthermore, the similar effects observed upon metal binding and the removal of His imidazole group suggest that the change in the local dynamics expected upon metal binding (*17*, *38*) are not a major factor in the observed decreases of $k_{H^+(1)}$ and $k_{H^+(2)}$ (eqs 1 and 2).

An alternative mechanism for the effect of metal ion binding was proposed by Gerencsér and Maroti (*19*), who interpreted their results of the pH dependence of metal binding as arising from changes of the pK_as of internal acid residues that are responsible for proton transfer. Our results suggest only minor changes in the pK_as of internal groups (as discussed above)[4] that are insufficient to account for the observed change in the proton-transfer rate. In addition, the presence of a protonated His is consistent with the small increases in k_{BD} observed in the His mutants (Table 1) due to the loss of a positive charge at a long distance from Q_B (~20 Å). Therefore, removing the two histidine imidazole groups *decreases* the local positive charge whereas binding of Zn^{2+} or Cd^{2+} *increases* the local positive charge. Thus, the electrostatic interaction would lead to different results

[4] The titration of k_{BD} at low pH is sensitive to the ionization state of the pathway components Asp-L210, Asp-M17 (*16*), and Asp-L213 (*13*), and the titration at high pH is sensitive to the ionization state of Glu-L212 (*3*, *4*). Neither of these titrations are affected in the double mutant RC (data not shown), suggesting that there are no major changes in the pK_as of these carboxylic acids. The apparent pK_a of Glu-L212 based on the k_{BD} data (not shown), as defined by the onset of the higher pH titration, is approximately 9.3 for both the native and mutant RCs. This agrees well with the values of 9.5−9.8 reported in the literature (*3*, *4*, *28*), accounting for a slight shift due to the different detergent and salt concentrations used in this study. Note that this pK_a is greater than the apparent pK_a determined from the $k_{AB}^{(1)}$ data as has been observed previously (*3*, *4*, *28*). The reason for this difference is not determined but could involve different couplings with other groups resulting from the different time scales of the measurements (~1 ms for $k_{AB}^{(1)}$ and ~1 s for k_{BD}). In addition, the Q_B movement associated with its reduction could contribute differently to the two reactions which would change the energy required to protonate Glu-L212 (*35*, *36*).

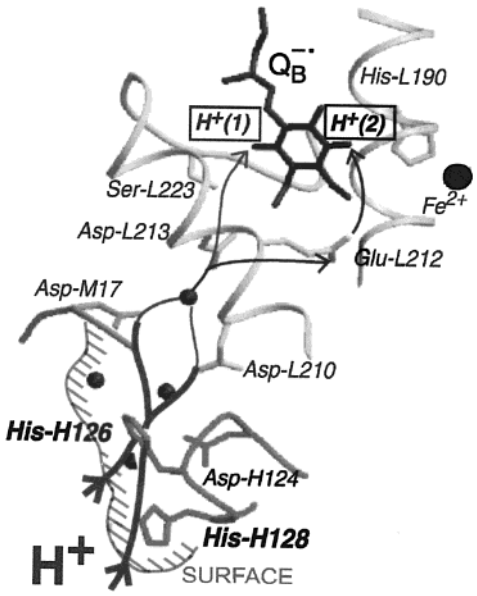

FIGURE 6: Part of the structure of the RC in the charge-separated state (coordinates from ref *57*). Shown are the secondary quinone, Q_B, and the amino acid residues that are important for transfer of $H^+(1)$ and $H^+(2)$ to Q_B. Water molecules are indicated by small spheres. The RC surface, indicated in the figure, was defined by the van der Waals radii of the surface-accessible atoms. The parallel pathways through His-H126 or His-H128 as well as through Asp-M17 or Asp-L210 (*16*) are indicated by heavy lines. $H^+(1)$ is taken up from solution and transferred to Q_B concomitant with $k_{AB}^{(2)}$. $H^+(2)$ is taken up from solution and transferred to Glu-L212 during $k_{AB}^{(1)}$, and transferred on to Q_B following $k_{AB}^{(2)}$ (eq 2). $H^+(1)$ and $H^+(2)$ share the same pathway up to Asp-L213. The figure was prepared using the programs MOLSCRIPT (*58*), Raster3D (*59*), and Adobe Illustrator.

for metal ion binding and His replacement. This is in contrast to the finding that both removal of the imidazole groups at His-H126 and His-H128, and the binding of Zn^{2+} or Cd^{2+} result in the same rate-limiting proton-transfer step for $k_{AB}^{(1)}$ and $k_{AB}^{(2)}$. We therefore conclude that these His residues function as proton donors, which can be inactivated by either removal of the imidazole group or binding of a metal ion.

Proton-Transfer Pathway. Several proton-transfer pathways have been proposed (*9*−*11*), based on crystal structures and mutagenesis experiments. This led to the suggestion that proton transfer in the RC is a delocalized process, with multiple proton-transfer pathways acting in parallel (*19*). In this model, as discussed above, the effect of metal binding to the RC was proposed to be electrostatic in origin (*19*), resulting in pK_a changes of amino acids such as Asp-L213, which are common to all of the putative proton-transfer pathways. We do not favor this view as explained above, but instead propose that proton transfer in the RCs proceeds along well-defined dominant pathways that share a common entry point as shown in Figure 6.

The slow proton uptake in the double mutant HA(H126)/HA(H128) RC, and the rescue of the rates by addition of imidazole show that the His-H126 and His-H128 are important for fast protonation of Glu-L212 [uptake of H^+-(2) (eq 1)] and of $Q_B^{-\bullet}$[uptake of $H^+(1)$ (eq 2)]. Because the single His mutant RCs show no effects on the rates of $k_{AB}^{(1)}$ or $k_{AB}^{(2)}$, either one of these histidines can function as the "entry-point" for protons. We can now trace the transfer of protons from the surface of the RC onto both carbonyls of the Q_B molecule (see Figure 6): for the uptake of $H^+(1)$, the pathway starts at His-H126 or His-H128, proceeds via Asp-M17 and Asp-L210, which act cooperatively (*16*), Asp-L213 (*3*, *13*, *14*), Ser-L223 (*12*), and ends on the O1 carbonyl of the quinone. For the uptake of $H^+(2)$, the pathway shares the involvement of the same His and Asp residues, but branches at Asp-L213 (*16*), proceeding to Glu-L212 (*3*, *4*), and onto the O4 carbonyl of the quinone.

It is interesting to note that there is a redundancy of proton-transfer components at the beginning of the pathway at the cytoplasmic side. This is shown by the requirement for only one His (either His-H126 or His-H128) and one Asp (either Asp-M17 or Asp-L210) (*16*) for efficient proton transfer. Closer to the Q_B site, however, there is an obligatory requirement for the residues Asp-L213, Ser-L223 and Glu-L212. The pathways for $H^+(1)$ and $H^+(2)$ can thus be represented as "funnels", wide near the cytoplasmic entrance and narrowing as it gets closer to Q_B.

Special Role of Histidines in Proton Transfer. Histidines are commonly used as acid−base catalysts (proton donors/acceptors) in enzymes. Two examples of enzyme families in which a His is crucial for function are the serine proteases, where a histidine is part of the "charge relay" system that accepts a proton from the reactive serine (*40*), and carbonic anhydrases where reprotonation of the Zn^{2+}-bound hydroxide occurs by proton transfer from a histidine (*41*).

Histidine is an efficient proton donor because its pK_a is near the physiological pH of 7. Residues with a lower pK_a are predominantly ionized at pH 7 and are therefore not good proton donors. Residues with a higher pK_a will not readily transfer a proton since, according to the Brönsted relation, the proton-transfer rate decreases with increasing pK_a of the donor (*42*).

Histidines have also been proposed to form part of so-called "proton-collecting antennas" which facilitate rapid proton transfer into the interior of the protein (*39*). These "antennas" consist of surface acidic groups, e.g., carboxylates and histidines, that attract, retain and rapidly transfer protons from the surface of the protein to internal groups. Such acidic surface groups have been proposed to facilitate proton transfer in several proton-transferring enzymes, such as cytochrome *c* oxidase (*43*, *44*), bacteriorhodopsin (*45*), and the bacterial reaction center (*46*). The present work extends those ideas by providing experimental identification of surface histidines that could function in such a manner. It is worth noting that these two surface His are crucial for this function, as in their absence, no other surface groups provide an efficient alternative for proton transfer into the RC.

Metal Ion Binding in Other Biological Systems. Inhibition of the proton transfer by metal ion binding to the *Rb. sphaeroides* RC (*18*, *47*) is caused by coordination of the metal ion to His-H126 and His-H128 (*17*), thereby displacing protons on these histidines. This decreases the rates of proton transfer, which in turn decreases the rates of the measured electron transfers (*6*, *18*). A similar mechansim can explain the observed decrease in electron-transfer rates upon metal ion binding in *Rhodobacter capsulatus* and *Rhodopseudomonas viridis* RCs (*48*). In view of the high sequence similarity between *Rb. sphaeroides* and *Rb. capsulatus* RCs (*49*), a similar proton pathway is likely in the *Rb. capsulatus* RC. In the RC of *Rps. viridis* (*50*), the proton pathway differs (*51*), but there is an analogous His-acid motif (*17*) that could be responsible for the observed metal ion inhibition. Also

the distantly related RC from *Thermochromatium tepidum* (*52*) has a pair of histidines (His-H122 and His-M239) that, in analogy with *Rb. sphaeroides*, are likely to be at the entry point of the proton-transfer pathway to Q_B.

Divalent cations such as Zn^{2+} and Cd^{2+} have also been shown to inhibit the catalytic turnover in other proton-transferring proteins, including carbonic anhydrase (where it was shown that Cu^{2+} and Hg^{2+} bind to the histidine that reprotonates the Zn^{2+}-OH^-) (*53*), the cytochrome bc_1-complex (*54*), voltage-gated proton channels (*55*) and cytochrome *c* oxidase (*56*). In cytochrome *c* oxidase Zn^{2+} was suggested to bind to surface histidines close to the entrance of a proton-transfer pathway (*56*). In most of these systems, surface histidines seem to play an important role in proton transfer.

SUMMARY

We have shown by site-directed mutagenesis, combined with kinetic studies of the proton-coupled electron-transfer reactions $k_{AB}^{(1)}$ and $k_{AB}^{(2)}$, the involvement of the surface residues His−H126 and His−H128 in proton transfer to Q_B. Mutant RCs were constructed in which either one or both histidines were replaced with alanines. In the single His mutant RCs, no effects were observed on either $k_{AB}^{(1)}$ or $k_{AB}^{(2)}$. In contrast, in the double His mutant RC, both $k_{AB}^{(1)}$ and $k_{AB}^{(2)}$ were slowed, and were limited by proton uptake from solution. Fast proton uptake rates could be restored ('rescued') by the addition of exogenous proton donors such as imidazole. Thus, these His residues act as protein-bound proton donors at the entry point of the proton-transfer pathways.

ACKNOWLEDGMENT

We are grateful to Edward Abresch, Jeanette A. Johnson and Shannon Foster for expert technical assistance.

REFERENCES

1. Okamura, M. Y., Paddock, M. L., Graige, M. S., and Feher, G. (2000) *Biochim. Biophys. Acta 1458*, 148−163.
2. Blankenship, R. E., and Madigan, M. T., Bauer, C. E. (1995) *Anoxygenic photosynthetic bacteria*, Kluwer academic publishers, Dordrecht, The Netherlands.
3. Takahashi, E., and Wraight, C. A. (1992) *Biochemistry 31*, 855−866.
4. Paddock, M. L., Rongey, S. H., Feher, G., and Okamura, M. Y. (1989) *Proc. Natl. Acad. Sci. U.S.A. 86*, 6602−6606.
5. Graige, M. S., Feher, G., and Okamura, M. Y. (1998) *Proc. Natl. Acad. Sci. U.S.A. 95*, 11679−11684.
6. Ädelroth, P., Paddock, M. L., Sagle, L. B., Feher, G., and Okamura, M. Y. (2000) *Proc. Natl. Acad. Sci. U.S.A. 97*, 13086−13091.
7. Graige, M. S., Paddock, M. L., Bruce, J. M., Feher, G., and Okamura, M. Y. (1996) *J. Am. Chem. Soc. 118*, 9005−9016.
8. McPherson, P. H., Schönfeld, M., Paddock, M. L., Okamura, M. Y., and Feher, G. (1994) *Biochemistry 33*, 1181−1193.
9. Fritzsch, G., Kampmann, L., Kapaun, G., and Michel, H. (1998) *Photosynth. Res. 55*, 127−132.
10. Baciou, L., and Michel, H. (1995) *Biochemistry 34*, 7967−7972.
11. Abresch, E. C., Paddock, M. L., Stowell, M. H. B., McPhillips, T. M., Axelrod, H. L., Soltis, S. M., Rees, D. C., Okamura, M. Y., and Feher, G. (1998) *Photosynth. Res. 55*, 119−125.
12. Paddock, M. L., McPherson, P. H., Feher, G., and Okamura, M. Y. (1990) *Proc. Natl. Acad. Sci. U.S.A. 87*, 6803−6807.
13. Paddock, M. L., Rongey, S. H., McPherson, P. H., Juth, A., Feher, G., and Okamura, M. Y. (1994) *Biochemistry 33*, 734−745.
14. Takahashi, E., and Wraight, C. A. (1990) *Biochim. Biophys. Acta 1020*, 107−112.
15. Paddock, M. L., Feher, G., and Okamura, M. Y. (2000) *Proc. Natl. Acad. Sci. U.S.A. 97*, 1548−1553.
16. Paddock, M. L., Ädelroth, P., Chang, C., Abresch, E. C., Feher, G., and Okamura, M. Y. (2001) *Biochemistry 40*, 6893−6902.
17. Axelrod, H. L., Abresch, E. C., Paddock, M. L., Okamura, M. Y., and Feher, G. (2000) *Proc. Natl. Acad. Sci. U.S.A. 97*, 1542−1547.
18. Paddock, M. L., Graige, M. S., Feher, G., and Okamura, M. Y. (1999) *Proc. Natl. Acad. Sci. U.S.A. 96*, 6183−6188.
19. Gerencsér, L., and Maróti, P. (2001) *Biochemistry 40*, 1850−1860.
20. Silverman, D. N. (2000) *Biochim. Biophys. Acta 1458*, 88−103.
21. Hays, A. M. A., Vassiliev, I. R., Golbeck, J. H., and Debus, R. J. (1998) *Biochemistry 37*, 11352−11365.
22. Ädelroth, P., Paddock, M. L., Beatty, J. T., Feher, G., and Okamura, M. Y. (2001) *Biophys. J. 80*, 427a.
23. Keller, S., Beatty, J. T., Paddock, M. L., Breton, J., and Leibl, W. (2001) *Biochemistry 40*, 429−439.
24. Chen, X. Y., Yurkov, V., Paddock, M. L., Okamura, M. Y., and Beatty, J. T. (1998) *Photosynth. Res. 55*, 369−373.
25. Lee, J. K., Kiley, P. J., and Kaplan, S. (1989) *J. Bacteriol. 171*, 3391−3405.
26. Isaacson, R. A., Lendzian, E., Abresch, E. C., Lubitz, W., and Feher, G. (1995) *Biophys. J. 69*, 311−322.
27. Paddock, M. L., Senft, M. E., Graige, M. S., Rongey, S. H., Turanchik, T., Feher, G., and Okamura, M. Y. (1998) *Photosynth. Res. 55*, 281−291.
28. Kleinfeld, D., Okamura, M. Y., and Feher, G. (1984) *Biochim. Biophys. Acta 766*, 126−140.
29. Verméglio, A., and Clayton, R. K. (1977) *Biochim. Biophys. Acta 461*, 159−65.
30. Tiede, D. M., Vazquez, J., Cordova, J., and Marone, P. A. (1996) *Biochemistry 35*, 10763−10775.
31. Kleinfeld, D., Okamura, M. Y., and Feher, G. (1985) *Biochim. Biophys. Acta 809*, 291−310.
32. Sebban, P., Maróti, P., Schiffer, M., and Hanson, D. K. (1995) *Biochemistry 34*, 8390−8397.
33. Beatty, J. T., Paddock, M. L., Feher, G., and Okamura, M. Y. (2000) *Biophys. J. 78*, 339A.
34. Li, J., Gilroy, D., Tiede, D. M., and Gunner, M. R. (1998) *Biochemistry 37*, 2818−2829.
35. Grafton, A. K., and Wheeler, R. A. (1999) *J. Phys. Chem. 103*, 5380−5387.
36. Mulkidjanian, A. Y. (1999) *FEBS Lett. 463*, 199−204.
37. Earnhardt, J. N., Tu, C., and Silverman, D. N. (1999) *Can. J. Chem. 77*, 726−732.
38. Duda, D., Tu, C. K., Qian, M. Z., Laipis, P., Agbandje-McKenna, M., Silverman, D. N., and McKenna, R. (2001) *Biochemistry 40*, 1741−1748.
39. Gutman, M., and Nachliel, E. (1990) *Biochim. Biophys. Acta 1015*, 391−414.
40. Blow, D. M., Birktoft, J. J., and Hartley, B. S. (1969) *Nature 221*, 337−340.
41. Tu, C. K., Silverman, D. N., Forsman, C., Jonsson, B. H., and Lindskog, S. (1989) *Biochemistry 28*, 7913−7918.
42. Brönsted, J. N., and Pedersen, K. (1923) *Z. Phys. Chem. A108*, 185.
43. Marantz, Y., Nachliel, E., Aagaard, A., Brzezinski, P., and Gutman, M. (1998) *Proc. Natl. Acad. Sci. U.S.A. 95*, 8590−8595.
44. Karpefors, M., Ädelroth, P., Aagaard, A., Sigurdson, H., Ek, M. S., and Brzezinski, P. (1998) *Biochim. Biophys. Acta 1365*, 159−169.
45. Checover, S., Nachliel, E., Dencher, N. A., and Gutman, M. (1997) *Biochemistry 36*, 13919−13928.

46. Gopta, O. A., Cherepanov, D. A., Junge, W., and Mulkidjanian, A. Y. (1999) *Proc. Natl. Acad. Sci. U.S.A. 96*, 13159−13164.
47. Utschig, L. M., Ohigashi, Y., Thurnauer, M. C., and Tiede, D. M. (1998) *Biochemistry 37*, 8278−8281.
48. Utschig, L. M., Poluektov, O., Schlesselman, S. L., Thurnauer, M. C., and Tiede, D. M. (2001) *Biochemistry 40*, 6132−6141.
49. Youvan, D. C., Bylina, E. J., Alberti, M., Begusch, H., and Hearst, J. E. (1984) *Cell 37*, 949−957.
50. Deisenhofer, J., Epp, O., Miki, K., Huber, R., and Michel, H. (1984) *J. Mol. Biol. 180*, 385−398.
51. Rongey, S. H., Paddock, M. L., Feher, G., and Okamura, M. Y. (1993) *Proc. Natl. Acad. Sci. U.S.A. 90*, 1325−9.
52. Nogi, T., Fathir, I., Kobayashi, M., Nozawa, T., and Miki, K. (2000) *Proc. Natl. Acad. Sci. U.S.A. 97*, 13561−13566.
53. Eriksson, E. A., Jones, T. A., and Liljas, A. (1986) *in Zinc Enzymes* (Bertini, I., Luchinat, C., Maret, M., Zeppzauer, M., Eds.) Birkhauser, Boston, 317−328.
54. Link, T. A., and von Jagow, G. (1995) *J. Biol. Chem. 270*, 25001−25006.
55. DeCoursey, T. E., and Cherny, V. V. (2000) *Biochim. Biophys. Acta 1458*, 104−119.
56. Aagaard, A., and Brzezinski, P. (2001) *FEBS Lett. 494*, 157−160.
57. Stowell, M. H., McPhillips, T. M., Rees, D. C., Soltis, S. M., Abresch, E., and Feher, G. (1997) *Science 276*, 812−816.
58. Kraulis, P. J. (1991) *J. Appl. Crystallogr. 24*, 946−950.
59. Merritt, E. A., and Bacon, J. D. (1997) *Methods Enzymol. 277*, 505−524.

BI011585S